

Article

Thermal Field Simulation and Optimization of PbF₂ Single Crystal Growth by the Bridgman Method

Lin Li ^{1,2,3}, Peixiong Zhang ^{1,2,3,*}, Zhen Li ^{1,2,3} and Zhenqiang Chen ^{1,2,3,*}¹ College of Physics & Optoelectronic Engineering, Jinan University, Guangzhou 510632, China² Guangdong Provincial Engineering Research Center of Crystal and Laser Technology, Guangzhou 510632, China³ Guangdong Provincial Key Laboratory of Optical Fiber Sensing and Communications, Guangzhou 510632, China

* Correspondence: pxzhang@jnu.edu.cn (P.Z.); tzqchen@jnu.edu.cn (Z.C.)

Abstract: PbF₂ single crystals are usually grown in the temperature gradient region by the Bridgman–Stockbarger method. Temperature distribution during the growth process is particularly important for the preparation of high-quality crystals. In this study, the temperature field during the growth of the PbF₂ single crystals was simulated based on the finite element method. The temperature distribution and temperature gradient changes in the crucible were investigated at different growth stages, including the seeding, shouldering, and iso-diameters stages. The calculated results show that as the crucible position continues downward during the growth process, the axial temperature gradient increases and then decreases from the bottom to the top of the crucible, with almost flat isotherms near the solid–liquid interface where the axial temperature gradient is larger. At the shoulder below the crucible, the solid–liquid interface was improved by adjusting the tilt angle. Furthermore, based on a novel design of the heat-insulating baffle, the concave solid–liquid interface in the iso-diameter stage can be effectively adjusted to realize a lower radial temperature gradient. This study provides theoretical guidance for the optimization of the growth of high-quality PbF₂ crystals by the Bridgman method.

Keywords: Bridgman–Stockbarger method; PbF₂ single crystal; finite element method; temperature distribution; solid–liquid interface



Citation: Li, L.; Zhang, P.; Li, Z.; Chen, Z. Thermal Field Simulation and Optimization of PbF₂ Single Crystal Growth by the Bridgman Method. *Crystals* **2024**, *14*, 473. <https://doi.org/10.3390/cryst14050473>

Academic Editor: Rainer Niewa

Received: 16 April 2024

Revised: 3 May 2024

Accepted: 4 May 2024

Published: 17 May 2024



Copyright: © 2024 by the authors. Licensee MDPI, Basel, Switzerland. This article is an open access article distributed under the terms and conditions of the Creative Commons Attribution (CC BY) license (<https://creativecommons.org/licenses/by/4.0/>).

1. Introduction

Fluoride crystals are excellent media for laser operations because of their wide transmission spectrum range, low refractive index, and low phonon energy [1–4]. Lead fluoride (PbF₂) crystals are a cubic crystalline system with excellent physicochemical properties and have been widely studied in recent years [5]. The PbF₂ crystals exhibit a high refractive index (1.82) and a wide band gap (5.07 eV), providing an excellent Cherenkov radiator [6]. Moreover, the melting point of PbF₂ is low (1100 K), and its solubility in water is only 6.4×10^{-2} g/100 g, which is significantly lower than that of materials such as BaF₂ and LiF, allowing its stable existence in air. The PbF₂ crystal, as a result of its abundant raw materials and low cost, is a fluoride crystal with an excellent overall performance. Compared with CaF₂, SrF₂, and other fluorides, PbF₂ has a lower phonon energy of 257 cm⁻¹, which gives it a longer energy level lifetime and makes it more favorable to be used as an ideal, high-efficiency laser matrix material.

The Vertical Bridgman (VB) method is usually used to grow PbF₂ crystals. The VB method is a crystal preparation method invented and perfected by Bridgman and Stockbarger et al. in 1925 and 1936, respectively [7,8]. It uses externally heated and melted solids inside the crucible to form a stable solid–liquid (S–L) interface at the interface between the melt and the crystals by designing a suitable temperature gradient environment. In the crucible, there are high-temperature, temperature gradient, and low-temperature zones

from top to bottom. As the crucible continues to move in a vertical downward direction, the formed S-L interface and temperature distribution changes. In the areas with large temperature gradients, the melt can be driven to solidify to the crystal and simultaneously affects the temperature field distribution by releasing heat and changing the ratio of the melt/crystal existence [9–11]. Therefore, the conditions of the temperature field are one of the crucial conditions that ensures the normal growth of crystals in the actual crystal growth. If the temperature field conditions cannot match the requirements of the crystal growth on the thermal environment, it will directly lead to the generation of streaks and cracks, and the grown crystals will have many defects. These defects may restrict the higher demand for crystals in high-tech fields and affect their industrial applications [12,13]. Consequently, it is important to reduce crystal defects, improve the controllability of crystal growth, and further explore the conditions to improve the quality and yield of crystal growth.

In the 1950s, the simulation of the unstable radial and linear flows in the gas phase by G.H. Bruce and D.W. Peaceman et al. [14] marked the advent of numerical simulation techniques. In the current crystal growth field, simulation has become an integral part of engineering design and optimization. Traditional experimental research usually tends to be more macroscopic and easily limited by experimental conditions, which is not conducive to the repeatable qualitative study of growth patterns. Numerical simulation software can be used to calculate in advance. While the process is unqualified, only the relevant improvement of each parameter condition in the model is needed and verified by calculations. Various physical problems can be solved through numerical calculations and the display of visual graphical results, which can improve research efficiency, save costs, and provide theoretical guidance for the subsequent growth of crystals [15–17].

At present, many domestic and foreign scholars are committed to studying the temperature field system of the crystals grown through the VB method. S.H. Hahn and J.K. Yoon [18] used numerical analysis to study the VB crystal growth and designed a reflector with a tilt angle of 37° to realize the transition of the S-L interface shape from concave to convex. Lu et al. [19] showed changes in the temperature field of VB-grown CaF_2 crystals and the effect of different temperature gradients on the S-L interface. X Yang et al. [20] investigated the influence of heat transfer characteristics on the vacuum-directed solidification process at different drop rates in the VB system and proposed a scheme to optimize the growth of polysilicon by using a slow and then a quick drop of the crucible. A.G. Ostrogorsky et al. [21] obtained a convex S-L interface and excellent radial uniformity by designing a rotating immersed thermal insulation baffle. Yingwu Jiang et al. [9] explored the effects of the low-temperature zone, cooling water, and furnace rise rate on the temperature field of a LiH single crystal grown through the VB method. In general, the stable and suitable temperature fields and S-L interface have crucial roles in the growth of high-quality crystals. However, there have not been any systematic studies on the S-L interface and the temperature gradients in the axial and radial inside the crucibles at different growth stages for growing PbF_2 crystals via the VB method. The optimized design regarding the adjustment of the crucible shape and baffle shape to the S-L interface at different growth stages needs to be further developed. The VB crystal growth method has the feature that the crucible can be self-designed, and the growth process is automated and simple, which allows directional growth by pretreatment at the bottom of the crucible [22]. Nonetheless, in the experiment, the crystals were grown in a closed crucible, leading to inconvenient direct observation of the crystal growth, which is not conducive to the control of the whole crystal growth process. After the traditional theoretical analysis and practical experiment, the research method that combines theoretical calculations and traditional experiments has been increasingly favored by domestic and foreign researchers and has become one of the important tools for the development of modern science and technology [23–25].

In short, the growth of PbF_2 single crystals depends on the temperature field distribution and the regulation of the S-L interface. This work takes the VB growth furnace as a background to establish a systematic radiative heat transfer model for simulating the temperature field of PbF_2 single-crystal growth. The temperature field inside the crucible

at different stages and the distribution of the temperature gradient at different positions during the crystal growth process were investigated to analyze the shape and to change the rules of the S-L interface. In addition, after designing the crucible shape and the shape of the heat-insulating baffle, the concave S-L interfaces in the shouldering and iso-diameter stages were improved. Control of the temperature field at different stages during the crystal growth through the VB method was achieved, providing theoretical guidance for higher quality PbF_2 crystal growth experiments.

2. Model and Methods

2.1. Bridgman–Stockbarger Model

The device diagram of the VB growth system is shown in Figure 1. It is mainly composed of a temperature-controlled thermocouple, alumina insulation, a descending rod, 304 stainless steel plate, and a vacuum system.

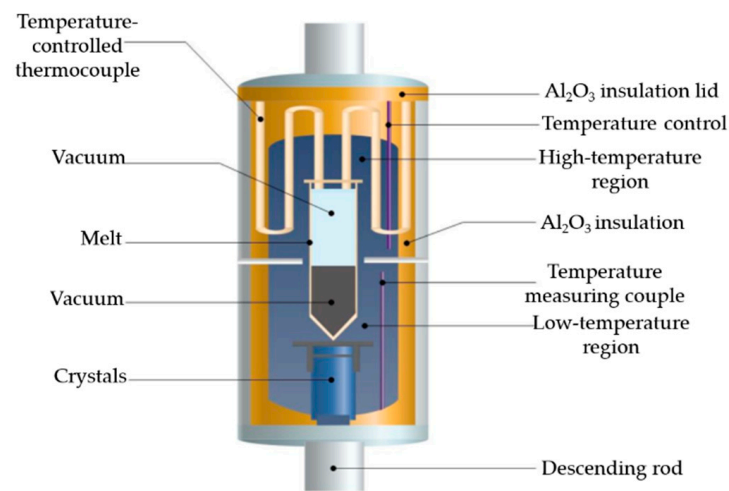


Figure 1. Schematic diagram of the Bridgman–Stockbarger method used to prepare PbF_2 crystals.

The specific growth process is as follows:

- (1) Furnace loading: The graphite crucible with well-mixed raw materials was placed in the corundum tube. After sealing, the tightness of the furnace was checked and the tube was pumped to a vacuum using a mechanical pump.
- (2) Growth: First, the temperature was set at 200 °C for 4 h to exclude the moisture in the raw material. Then, the temperature was increased to 980 °C, and after 1 h at a constant temperature, the furnace tube in which the crucible was located was slowly lowered at a rate of 0.5 mm/h, so that the polycrystalline material began to solidify and to grow in the temperature gradient zone.
- (3) Post-processing: When the graphite crucible descended to a predetermined height, its descent was stopped, and it was cooled down to room temperature at a cooling rate of 20–25 °C/h. The graphite crucible was then annealed at a constant temperature of 620 °C for 20 h to reduce the thermal stresses generated during the crystal growth.

2.2. Simulation Methods

Based on the crucible descent method of the crystal growth furnace designed by our laboratory, a corresponding simulation model was established. Considering the basically symmetric distribution of the whole furnace device, a 2D axisymmetric model was created to improve the calculation efficiency. Figure 2 shows a schematic diagram of a 2D axially symmetric model. The r is the length along the radial direction of the crucible, and the axial length of the crucible is 10 cm. The raw material was placed in a graphite crucible with a low thermal conductivity; the thermal barrier was carbon felt; and a water cooler made of stainless steel was located underneath the crucible. During the growth, the surroundings

of the crucible were evacuated to a vacuum. A heating source was only provided above the thermal barrier but not in the low-temperature zone, which ensured that the temperature gradient in the high-temperature region was smaller than the low-temperature region, thereby forming flat or convex S-L interfaces. This calculation studies the thermal field of the crucible at different positions as the growth progresses. There are growth stages from the seeding and shouldering to three different positions of the iso-diameters, corresponding to the axial coordinates of the start of the crucible in the order of 9.5, 8.5, 7, 5.5, and 4.5 cm. The outermost layer was an alumina insulation layer to reduce the heat loss from the furnace and to facilitate the formation of a symmetrical and uniform temperature gradient field. The outer wall of the entire temperature field was made of 304 stainless steel plate to form a box to protect the entire machine and to support the internal circuitry and mechanical structure.

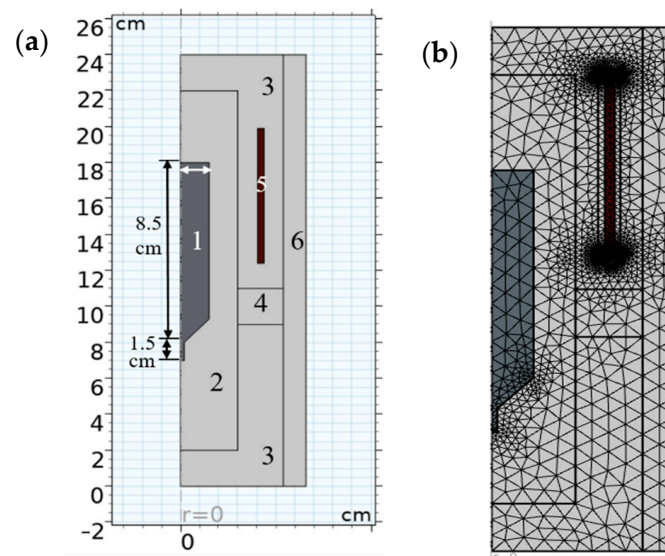


Figure 2. Structure of PbF_2 single crystal growth device. (a) A 2D axisymmetric structure (1, graphite crucible; 2 and 3, vacuum; 4 insulating baffle; 5 heater; 6, alumina insulation layer); and (b) a divided grid.

Finite element grids can be used to characterize the geometry and the solution domains, discretizing large regions into smaller units based on the geometry. The size and shape of the grid units usually affects the numerical stability of the model. This study exploited the physical field control grids, as shown in Figure 2b. The complete grid contained 7351 triangle domain units, 559 boundary units, and 45 vertex units. The average unit quality was 0.8379, and the grid area totaled 158.4 cm^2 . It can be seen that under the adaptive grid refinement process, the grid in the boundary and minor geometric regions is denser. It can be seen that under the adaptive grid refinement process, the grids in the boundary and fine geometric regions are denser, which is due to the larger error at this location, so the software can effectively improve the accuracy of the calculation by re-gridding the geometry using more refined units based on the initial grid and subsequently re-solving the model based on the new grids.

In this study, the temperature distribution at the symmetry axis ($r = 0$) is axisymmetric, and the diffusion equation for the radiative heat flux is as follows [26,27]:

$$q_{r,\lambda} = -\frac{4\pi}{3\beta\lambda} \nabla I_{b,\lambda} \quad (1)$$

The heat flux of the radiation depends on the temperature gradient and can be expressed as follows:

$$q_r = -K_r \nabla T \quad (2)$$

where K_r is the highly nonlinear coefficient of conductivity. The formula for the radiative heat transfer is as follows:

$$K_r = \frac{16n^2\sigma T^3}{3\beta_r} \quad (3)$$

where β_r is the Rosseland average extinction coefficient, σ is the scattering coefficient, and n is the refractive index. In the process of heat transfer in a solid, the temperature (T) is the dependent variable. The heat transfer equation for the temperature field is as follows:

$$\rho C_p \frac{\partial T}{\partial t} + \rho C_p \vec{u} \cdot \nabla T + \nabla \cdot \vec{q} = Q + Q_{ted} \quad (4)$$

$$\vec{q} = -k\nabla T \quad (5)$$

where the thermal conductivity k and density ρ are determined by the properties of each material. When the pressure or volume is fixed, the constant pressure heat capacity C_p varies with T . Heat transfer occurs in a fluid flowing with a certain velocity, and the vector \vec{u} is the velocity field in the thermal convective conduction mechanism. The heat transfer equation is used to express the dependence of the temperature on space and time in the solution area. The following equation is the basic form of its transient state:

$$\frac{\partial T}{\partial t} + \nabla \cdot (-k\nabla T) = 0 \quad (6)$$

The equation is a typical parabolic partial differential equation whose solution has the characteristic of initial temperature smoothing, which means that the heat is conducted from high to low.

This study uses the commercial software COMSOL 5.6 to simulate the thermal field distribution in the growth of PbF_2 single crystals by the heat exchange crucible descent method [28], which mainly involves the modules of radiative and solid heat transfer in the participating medium. A parametric solver and adaptive grid dissection are used to solve the temperature field and solid–liquid interface variations in the crucible at different growth stages.

3. Results and Discussion

3.1. Effect of the Crucible Structure on the S-L Interface in the Shouldering Stage

Three different solid–liquid interface types may be formed when growing PbF_2 crystals with the VB method, namely, convex, flat, and concave interfaces. The temperature of the melt above the interface and around the crucible is higher than the melting point, which is a convex interface. A concave interface appears when the temperature around the crucible is lower than the center of the crucible. While the temperature around the crucible is equal to that inside, the heat flow passes axially inside the crucible, which is a flat interface. The S-L interface during the crystal growth should be as slightly convex or ideally flat as possible, otherwise the quality of the crystals may be reduced or there might even be crystal burst. To achieve high-quality crystals, we first adjusted the shape of the crucible shoulder at the beginning of the growth.

The melting point of PbF_2 is about 827°C , which is 1100 K. Figure 3 shows the position and shape of the S-L interface at the bottom of the crucible with different shouldering angles and lengths. It can be seen that before tuning the shape of the shoulder, the S-L interface was obviously concave and the arc length difference (ΔL) between the concave and flat interfaces was 0.19 cm. This is due to the fact that the slant shoulder at such an angle scatters more than it absorbs heat, which results in the overcooling of the crucible wall. Spontaneous nucleation may occur on the overcooled crucible wall, forming crystals on the wall. Therefore, the tilting length at the bottom of the crucible was adjusted to 45° to avoid such issues. Under identical conditions, the calculated S-L interface is shown on the right side of Figure 3. It is observed that the ΔL between the concave and flat interfaces

after the structural optimization was reduced to 0.08 cm, making the S-L interface almost flat, thus greatly improving the previous concave interface. The subsequent calculations were carried out on the basis of the optimized crucible shape.

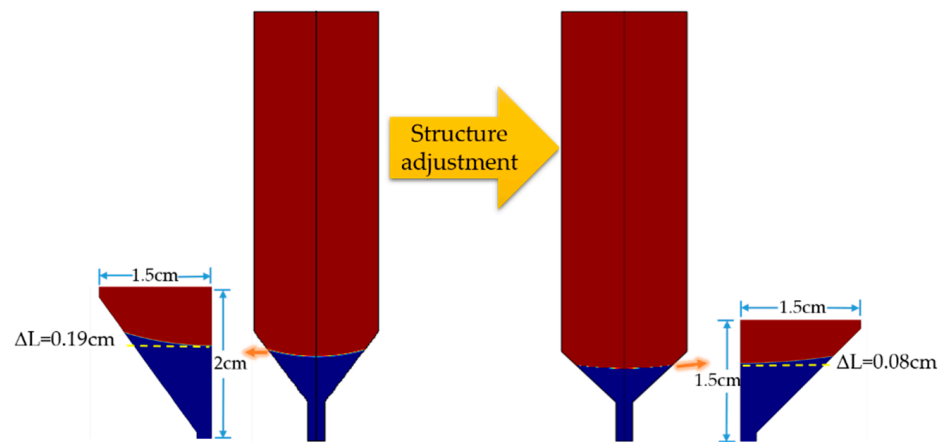


Figure 3. Shoulder position of the solid–liquid interface.

3.2. S-L Interface and Temperature Distribution in Different Stages

3.2.1. S-L Interface and Isothermal Distribution

In the crystal growth process of the VB method, a suitable temperature gradient is the basis for growing crystals, and it is necessary to take the temperature gradient and the descent position into account collectively. During the initial melting, the temperature inside the crucible should be raised above the melting point and kept constant for a while to ensure that the polycrystalline material is fully melted. As the heating time goes on, the crucible rises, and the temperature field and S-L interface position also change significantly. Therefore, based on the growth process of the crucible descent method, the temperature fields at different crucible positions, including the seeding, shouldering, and iso-diameter stages, were calculated separately. The results are shown in Figure 4, and the legend shows the distribution of the temperature values in K. After setting the heater program, the temperature inside the crucible rose. Since the crucible was positioned slightly above the heater at the start, the high temperature was distributed in the mid-upper part of the crucible. At the start of the seeding, due to the water cooling near the bottom and the good thermal conductivity of the graphite crucible, the isotherms in the crucible were ideally convex at the top and flat at the S-L interface at the bottom. With the time of heating, the crucible moved upward and the S-L interface moved to the shoulder of the crucible. It can be seen that through the previous optimization of the crucible tilt angle, the S-L interface turned flatter and the radial temperature gradient was smaller, which is conducive to high-quality crystal growth.

The iso-diameter growth stages are shown in Figure 4, 3.1–3.3. Since the crucible has moved downward, the highest temperatures are distributed above the crucible, while the low-temperature region is below the crucible. As the crystal keeps growing, the high-temperature region in the crucible becomes shorter, and the heating receptive surface gradually decreases. The part of the crucible in the low-temperature zone continues to lengthen, and the heat dissipation area gradually increases, which leads to reduced heating above the crucible and increased heat dissipation below it. This dynamic change process will affect the thermal balance within the crucible. It can be seen from Figure 4 that the position of the S-L interface of 3.1–3.3 gradually moves upward as the crucible continues to descend and changes from slightly concave to a flat interface.

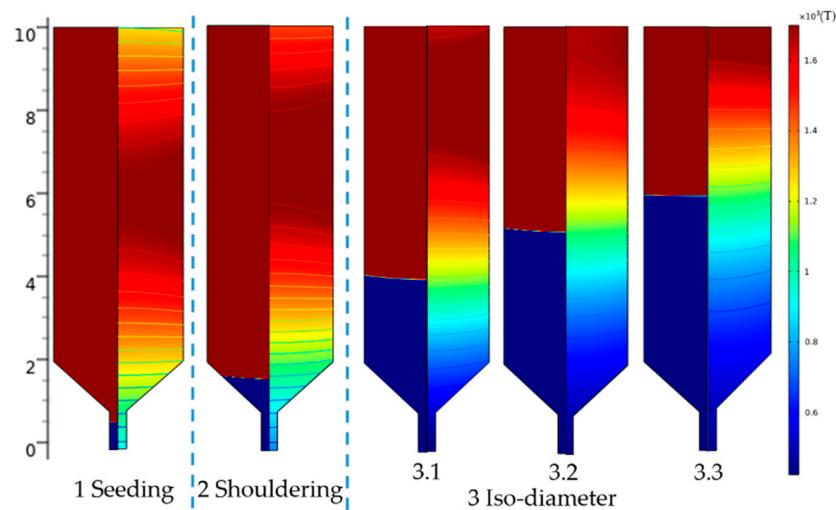


Figure 4. The distribution of the solid–liquid interface, temperature field, and isotherm at different positions in the crucible during the initial descending, shouldering, and iso-diameter stages.

3.2.2. Axial Temperature and Temperature Gradient

Figure 5 shows the temperature distribution from the bottom to the top of the crucible on the center axis of the crucible. As can be seen from Figure 5a, the highest temperature region gradually moves to the upper part of the crucible as the crucible position shifts upwards. The position of the S-L interface at 1100 K is also gradually shifted upward with the abscissa at 0.58 cm, 1.66 cm, 3.89 cm, 5.09 cm, and 5.93 cm, which correspond to the position of the S-L interface in Figure 4.

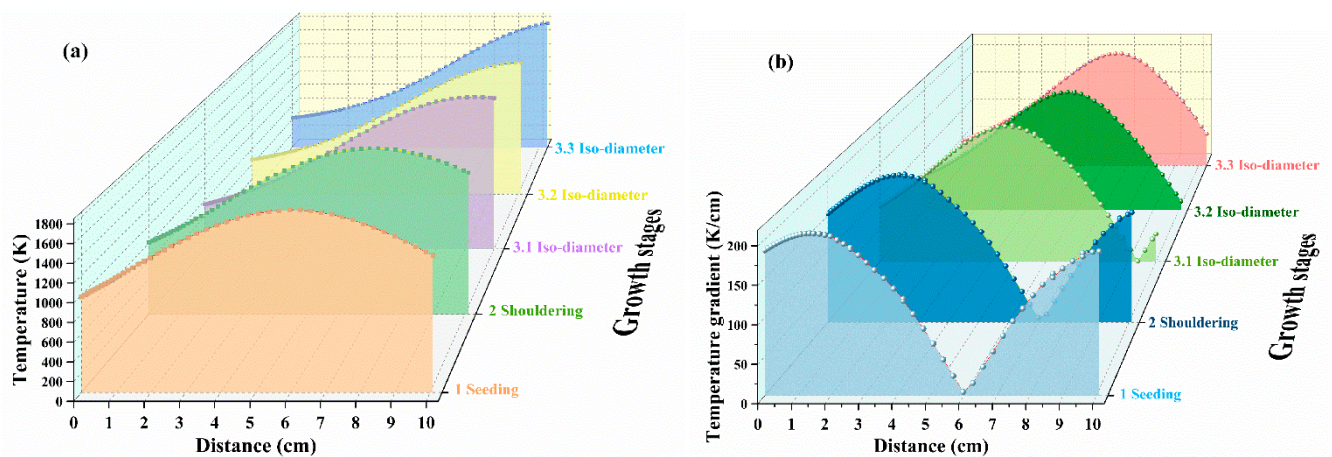


Figure 5. Axial temperature distribution at different positions of the crucible. (a) Temperature distribution, and (b) temperature gradient.

At conditions of thermal equilibrium, the growth rate of crystals is proportional to the temperature gradient. Therefore, maintaining a stable temperature gradient is an essential condition, especially at the S-L interface. If the temperature gradient in the growth region is too large, though the component overcooling can be suppressed, the large temperature gradient will make the just-grown crystals withstand a large temperature difference in short distances, which will result in a relatively large thermal stress, and will easily crack the crystals, thus being unfavorable to the control of the crystallization quality. As a result, while the temperature gradient is stable, a suitable temperature gradient should also be ensured to guarantee the smooth growth of the crystals.

During the crystal growth through the VB method, crystallization occurs near the S-L interface where there are large temperature gradients. The axial temperature gradient in

Figure 5b is calculated from Figure 5a. The S-L interface position in Figure 5a essentially agrees with the position of the maximum temperature gradient in Figure 5b, which is consistent with the actual growth. It can be seen that in the axis direction of the crucible center, although the temperature trend is basically rising gradually, the temperature gradient changes in a curvilinear manner. Especially at the beginning of the growth, since the crucible is located higher up in the furnace, the temperature at the top of the crucible decreases slightly in comparison to the region of the highest temperatures, and the associated temperature gradient increases again but is still smaller than the highest region of the temperature gradient in the crystallization position and does not interfere with the normal growth processes. While in the iso-diameters growth stages, the maximum temperature gradient region gradually moves toward the top of the crucible as the crucible position increases, which ensures the successful growth process of the crystals.

3.2.3. Radial Temperature Distribution at Different Positions

During the crystal growth, the crucible moves upward and the radial temperature inside the crucible changes. Moreover, the radial temperature distribution in the crucible varies in the upper, middle, and lower parts of the crucible at different growth stages. At different growth stages, the radial temperature distribution comparison at different locations in the crucible is shown in Figure 6. In the seeding, the temperature is generally a slightly concave isotherm with low, middle, and high edges. Moreover, the radial temperature gradient below the crucible is small and an almost flat isotherm. In the shouldering, the radial temperature in the bottom of the crucible is high in the center and low at the edges with a slightly convex isotherm. The radial temperature in the middle and top of the crucible is low in the center and high at the edges with a slightly concave isotherm.

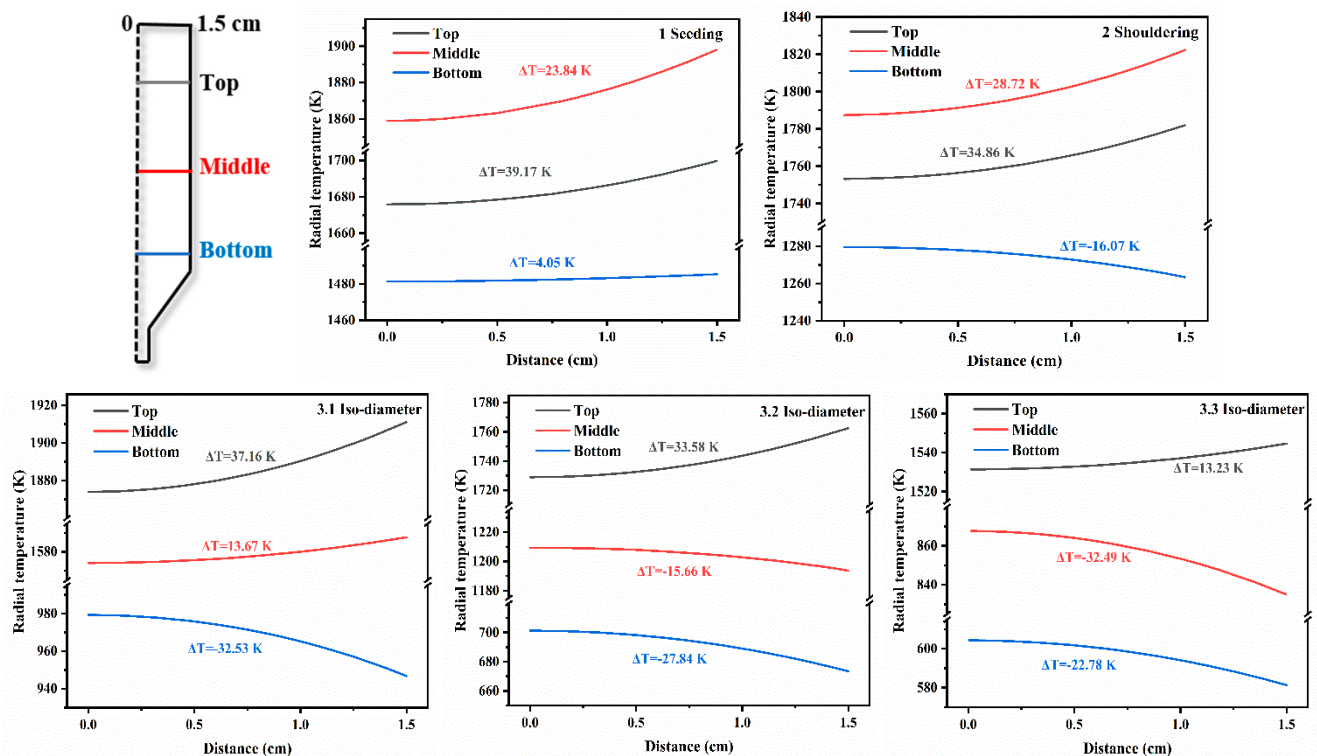


Figure 6. Radial temperature distribution at the top, middle, and bottom positions of the crucible in different growth phases.

As shown in Figure 5b, the crystallization region with a large temperature gradient on the axis in the isotropic growth stage of 3.1 and 3.2 is in the middle of the crucible, and

the region with a large temperature gradient in the isotropic stage of 3.3 is gradually closer to the top of the crucible. While the radial temperatures of the isotropic growth stage in 3.1 and 3.2 in Figure 6 indicate that the radial temperature difference in the middle of the crucible at this stage is -13.67 K and -15.66 K, respectively, the temperature gradients are both slightly smaller, which indicates that those isotropic temperatures are relatively flat. In the iso-diameter growth stage of 3.3, the absolute value of the temperature gradient in the middle of the crucible increases, but the growth region has been shifted to the top of the crucible at this period. The temperature distribution on top of the crucible in stage 3.3 shows a slightly convex isotherm with a low center and high edge. The maximum temperature difference is 13.23 K, which has a small temperature gradient and is favorable for the growth of crystals.

3.3. Effect of the Thermal Barrier Shape on the S-L Interface in the Iso-Diameter Stage

In the calculations of Section 3.2.1, the S-L interfaces are essentially flat, whereas the shape of the interface at the iso-diameter growth stage of 3.1 is still slightly concave. In order to explore the effect of the heat shield on the S-L interface at this stage, the shape of the insulating baffle was optimized, which is shown in Figure 7. The shape before the optimization of the insulating baffle was rectangular, corresponding to a concave S-L interface at stage 3.1, with a maximum distance of 0.14 cm in the axial direction. Due to the existence of the barrier, there is no direct radiant heating source, and the crucible dissipates massive heat from the upper to the lower cold cavities, causing overcooling on the crucible wall, which in turn produces a concave interface. S.H. Hahn et al. [21] found that the addition of a reflective screen with a certain inclination to the insulating baffle improves the shape of the S-L interface. Therefore, an insulating baffle with a certain tilting angle was designed, and the calculated results of the S-L interface shape under this condition are shown on the right side of Figure 7. Compared with the position and shape of the S-L interface before the optimization of the insulating baffle, it can be seen that the position of the interface is slightly decreased, which is due to the fact that a baffle with a certain slope can accommodate more heat in this region, so that the temperature at the S-L interface, which has a large temperature gradient, is slightly increased; therefore, the melting point of PbF_2 , 1100 K, can be reached at a lower position. Furthermore, after optimizing the shape of the baffle, the temperature of the crucible walls increased slightly due to the increase in the heat accommodation area near the underside of the baffle. As a result, the maximum axial distance difference of the S-L interface is shortened from 0.14 cm to 0.08 cm, and the radial temperature gradient is reduced, as shown in the calculation results in Figure 7. The above computational results demonstrate that the novel optimized insulating baffle improves the concave interface of the iso-diameter stages.

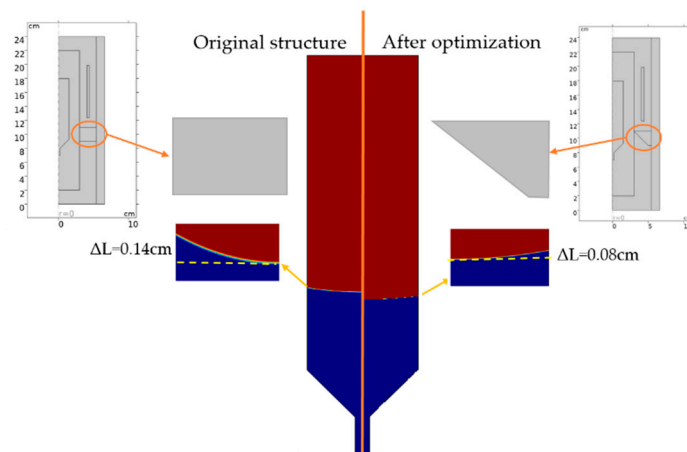


Figure 7. Effect of optimizing the structure of the thermal barrier on the S-L interface in the iso-diameter of the 3.1 stage.

4. Conclusions

In this paper, the growth of PbF₂ crystals through the VB method was investigated using numerical simulation and theoretical analysis, including the S-L interface and temperature field distribution in the crucible during different growth stages, such as the seeding, shouldering, and iso-diameters stages. By adjusting the tilting angle of the shoulder below the crucible, the S-L interface shape turned from concave to flat in the shouldering stage. The temperature distribution and temperature gradient distribution in the axial direction were also systematically analyzed, finding that the S-L interfaces were all distributed in a region with the larger temperature gradient and gradually moved to the position above the crucible during the growth process. Further, the radial temperature distributions in the top, middle, and bottom of the crucible at different growth stages were analyzed, and it was found that the radial temperature gradients at the S-L interface were all smaller at the iso-diameter growth stage, which is conducive to better crystallization at these growth stages. Additionally, to optimize the slightly concave S-L interface in the iso-diameter stage of 3.1, a novel design shape of the thermal barrier was designed, and its validity was verified via theoretical calculations.

Author Contributions: Conceptualization, P.Z. and Z.C.; methodology, L.L.; software, Z.C.; validation, P.Z.; formal analysis, L.L.; investigation, L.L.; resources, Z.L.; data curation, P.Z.; writing—original draft preparation, L.L.; writing—review and editing, P.Z.; visualization, L.L.; supervision, Z.L.; project administration, Z.L.; and funding acquisition, Z.C. All authors have read and agreed to the published version of the manuscript.

Funding: This research was funded by the National Natural Science Foundation of China (NSFC) (61935010, 51972149, and 62375106); the Science and Technology Program of Guangzhou (2024A03J0240); and the Key-Area Research and Development Program of Guangdong Province (2020B090922006).

Data Availability Statement: The original contributions presented in the study are included in the article, further inquiries can be directed to the corresponding authors.

Conflicts of Interest: The authors declare no conflicts of interest.

References

1. Ure, R.W., Jr. Ionic conductivity of calcium fluoride crystals. *J. Chem. Phys.* **1957**, *26*, 1363–1373. [[CrossRef](#)]
2. Stepanov, S.A.; Chinkov, E.P.; Shtan'ko. Time-resolved optical absorption measurements of calcium fluoride crystals. *Opt. Mater.* **2024**, *150*, 115271. [[CrossRef](#)]
3. Zhang, P.; Liao, J.; Niu, X.; Tan, H.; Li, S.; Zhu, S.; Yin, H.; Ma, F.; Yang, Q.; Hang, Y. Intense 2.1–4.2 μm broadband emission of Co/Er: PbF₂ mid-infrared laser crystal. *Opt. Lett.* **2021**, *46*, 3913–3916. [[CrossRef](#)]
4. Zhang, P.; Hang, Y.; Zhang, L. Deactivation effects of the lowest excited state of Ho³⁺ at 2.9 μm emission introduced by Pr³⁺ ions in LiLuF₄ crystal. *Opt. Lett.* **2012**, *37*, 5241–5243. [[CrossRef](#)]
5. Chen, Y.; Tan, J.; Zhang, P.; Zheng, W.; Li, L.; Zhang, L.; Li, Z.; Hang, Y.; Chen, Z. Influence of Nd³⁺ concentration on mid-infrared emission in PbF₂ crystal co-doped with Ho³⁺ and Nd³⁺ ions. *J. Rare Earth.* **2024**, *42*, 479–487. [[CrossRef](#)]
6. Cemmi, A.; Colangeli, A.; D'orsi, B.; Di Sarcina, I.; Diociaiuti, E.; Fiore, S.; Paesani, D.; Pillon, M.; Saputi, A.; Sarra, I. Radiation study of Lead Fluoride crystals. *J. Instrum.* **2022**, *17*, T05015. [[CrossRef](#)]
7. Bridgman, P.W. Certain physical properties of single crystals of tungsten, antimony, bismuth, tellurium, cadmium, zinc, and tin. In *Papers 32–58*; Harvard University Press: Cambridge, MA, USA, 1964; pp. 1851–1932.
8. Stockbarger, D.C. The production of large single crystals of lithium fluoride. *Rev. Sci. Instrum.* **1936**, *7*, 133–136. [[CrossRef](#)]
9. Jiang, Y.; Xie, D.; Wu, J.; Li, H.; Zhu, J.; Ni, M.; Gao, T.; Ye, X. Dynamic Simulation of the Temperature Field of LiH Single Crystal Growth. *Crystals* **2023**, *13*, 504. [[CrossRef](#)]
10. Mooney, R.P.; McFadden, S.; Gabalcová, Z.; Lapin, J. An experimental–numerical method for estimating heat transfer in a Bridgman furnace. *Appl. Therm. Eng.* **2014**, *67*, 61–71. [[CrossRef](#)]
11. Nefedov, O.; Dovnarovich, A.; Kostikov, V.; Mozhevitina, E.; Bocharnikov, D.; Avetissov, I. Numerical Simulation of CdTe Crystal Growth Using the Vertical Gradient Freeze Technique Assisted by Axial Low-Frequency Oscillations of the Melt. *Crystals* **2024**, *14*, 72. [[CrossRef](#)]
12. Ouyang, H.; Shyy, W. Numerical simulation of CdTe vertical Bridgman growth. *J. Cryst. Growth* **1997**, *173*, 352–366. [[CrossRef](#)]
13. Crocco, J.; Bensalah, H.; Zheng, Q.; Carcelén, V.; Diéguez, E. Influence of SiC pedestal in the growth of 50 mm CZT by Vertical gradient freeze method. *J. Cryst. Growth* **2012**, *360*, 92–94. [[CrossRef](#)]
14. Bruce, G.H.; Peaceman, D.; Rachford, H., Jr.; Rice, J.J. Calculations of unsteady-state gas flow through porous media. *J. Pet. Technol.* **1953**, *5*, 79–92. [[CrossRef](#)]

15. Zhang, S.; Li, T.; Li, Z.; Sui, J.; Zhao, L.; Chen, G. Thermal field design of a large-sized SiC using the resistance heating PVT method via simulations. *Crystals* **2023**, *13*, 1638. [[CrossRef](#)]
16. Xu, Z.; Zhang, J.; Cao, Z.; Lu, W.; Liu, H. Study on Thermal Field of Growth System of CdZnTe Crystal Growth by Traveling Heater Method. *J. Synthetic. Cryst.* **2023**, *52*, 1589–1598. (In Chinese)
17. Zhao, G.; Qu, L.; Li, J.; Ma, R. Numerical Simulation of Stress Intensity Factor for Pore-Crack in Quartz Crucible under High Temperature Cyclic Loading. *J. Synthetic. Cryst.* **2023**, *52*, 493–500. (In Chinese)
18. Hahn, S.; Yoon, J. Numerical analysis for the application of radiative reflectors to vertical Bridgman growth configurations. *J. Cryst. Growth* **1997**, *177*, 296–302. [[CrossRef](#)]
19. Lu, W.-Q. Boundary element analysis of the heat transfer in Bridgman growth process of semi-transparent crystals. *Mater. Sci. Eng. A-Struct.* **2000**, *292*, 219–223. [[CrossRef](#)]
20. Yang, X.; Lv, G.; Ma, W.; Xue, H.; Chen, D. The effect of radiative heat transfer characteristics on vacuum directional solidification process of multicrystalline silicon in the vertical Bridgman system. *Appl. Therm. Eng.* **2016**, *93*, 731–741. [[CrossRef](#)]
21. Ostrogorsky, A.; Riabov, V.; Dropka, N.J. Interface control by rotating submerged heater/baffle in vertical Bridgman configuration. *J. Cryst. Growth* **2018**, *498*, 269–276. [[CrossRef](#)]
22. Chang, C.J.; Brown, R.A.J. Radial segregation induced by natural convection and melt/solid interface shape in vertical Bridgman growth. *J. Cryst. Growth* **1983**, *63*, 343–364. [[CrossRef](#)]
23. Nefedov, O.; Dovnarovich, A.; Kostikov, V.; Levonovich, B.; Avetissov, I. Axial Vibration Control Technique for Crystal Growth from the Melt: Analysis of Vibrational Flows' Behavior. *Crystals* **2024**, *14*, 126. [[CrossRef](#)]
24. Li, J.C.; Li, Z.Y.; Liu, L.J.; Wang, C.Z.; Jin, Y.Q. Effects of melt depth on oxygen transport in silicon crystal growth by continuous-feeding Czochralski method. *J. Cryst. Growth* **2023**, *610*, 127180. [[CrossRef](#)]
25. Sinehbaghizadeh, S.; Saptoro, A.; Amjad-Iranagh, S.; Naeiji, P.; Tiong, A.N.T.; Mohammadi, A.H. A comprehensive review on molecular dynamics simulation studies of phenomena and characteristics associated with clathrate hydrates. *Fuel* **2023**, *338*, 127201. [[CrossRef](#)]
26. Vajdi, M.; Moghanlou, F.S.; Sharifianjazi, F.; Asl, M.S.; Shokouhimehr, M.J. A review on the Comsol Multiphysics studies of heat transfer in advanced ceramics. *J. Compos. Compd.* **2020**, *2*, 35–43. [[CrossRef](#)]
27. Cuevas, J.C.; García-Vidal, F.J. Radiative heat transfer. *ACS Photonics* **2018**, *5*, 3896–3915. [[CrossRef](#)]
28. Pryor, R.W. *Multiphysics Modeling Using COMSOL®: A First Principles Approach*; Jones & Bartlett Publishers: Burlington, MA, USA, 2009.

Disclaimer/Publisher's Note: The statements, opinions and data contained in all publications are solely those of the individual author(s) and contributor(s) and not of MDPI and/or the editor(s). MDPI and/or the editor(s) disclaim responsibility for any injury to people or property resulting from any ideas, methods, instructions or products referred to in the content.